

# Muscle Activity Analysis using Higher-Order Tensor Models: Application to Shared Muscle Synergy Identification

Ahmed Ebied<sup>1,\*</sup>, Eli Kinney-Lang<sup>1</sup>, Loukianos Spyrou<sup>1</sup>, Javier Escudero<sup>1</sup>,

**1 the Institute for Digital Communications, School of Engineering,  
University of Edinburgh, Edinburgh EH9 3FB, United Kingdom**

\* [ahmed.ebied@ed.ac.uk](mailto:ahmed.ebied@ed.ac.uk)

## Abstract

*Objective:* Higher-order tensor decompositions have hardly been used in muscle activity analysis despite the fact that multichannel electromyography (EMG) datasets used in muscle synergy studies naturally present multi-way structure. Here, we seek to discuss and demonstrate the potential of tensor decomposition as a framework to estimate muscle synergies from 3<sup>rd</sup>-order EMG tensors constructed by stacking repetitions of multi-channel EMG for several tasks. *Methods:* We compare the two most common decomposition models – Parallel Factor Analysis (PARAFAC) and Tucker – in muscle synergy extraction from the three main degrees of freedom (DoF) of the wrist using the first Ninapro database. We then utilise the power tensor factorisation to create a novel direct method for shared and task-specific synergy estimation from two biomechanically related tasks by developing a constrained Tucker decomposition method. Our approach is compared with the current standard approach of repetitively applying non-negative matrix factorisation (NMF) to a series of the movements. *Results:* The results show that the constrained Tucker method successfully identified the shared and task-specific synergies for all 3 DoF tensors directly and it was robust to misassignments with regard to task-repetition information unlike NMF, thanks to exploring the multi-way structure of muscle activity. *Conclusions:* We showed the potential of tensor factorisations to study and characterise muscle activity and developed a new direct method for shared and task-specific synergy identification with a constrained Tucker decomposition. *Significance:* We expect that this study will pave the way for the development of muscle activity analysis methods based on higher-order techniques.

## 1 Introduction

Higher-order tensors are the generalisation of vectors (1<sup>st</sup>-order tensors) and matrices (2<sup>nd</sup>-order tensors). When analysing higher-order data, tensor decompositions provide several advantages, such as compactness, uniqueness of decomposition and generality of the identified components, over matrix factorisations [11]. Tucker [50] and Parallel Factor Analysis (PARAFAC) [24] decompositions are the most common methods to factorise the tensor into its main components. In general, PARAFAC (also known as Canonical Polyadic Decomposition CANDECOMP) provides uniqueness to the solution as it is a special case of the Tucker method, which provides more flexibility than PARAFAC. In the recent years, higher-order tensor decomposition has received substantial attention in signal processing applications and has been utilised frequently

in brain activity analysis [15]. It has been applied on EEG data to classify epileptic patients [42] and for source localisation [5] in addition to MEG for Alzheimer's disease diagnosis [23]. However, it has only been used in two recent studies on muscle activity. We classified between wrist movements using the components of a 4<sup>th</sup>-order muscle activity tensor to provide a proof-of-concept for this approach [22]. Another study [51] used tensor factorisation for feature extraction from a 2-channel electromyograms (EMGs) for classification.

Usually, the multichannel EMG data are represented in the form of matrix with channels and time as indices and two-way signal processing methods have been prominent for muscle activity analysis. However, in most EMG studies, data are naturally structured with more modes than the temporal and space indices. For instance, the EMG datasets usually includes repetitions of subjects and/or movements. This means that the muscle activity naturally fit into a higher-order tensor model including additional modes to the temporal and spatial. This is what the seminal studies [22, 51] illustrated and shows that current 2<sup>nd</sup>-order approaches do not take advantage of the natural data structure. Actually, procedures often include a repetitive application of 2<sup>nd</sup>-order analysis. This means that some information about the interaction between modes may be lost in those approaches. Therefore, the first objective of this study is to demonstrate the use of higher-order tensor decomposition in muscle activity analysis by highlighting the differences between PARAFAC and Tucker models in muscle synergy extraction.

An important concept in the analysis of muscle activity is the muscle synergy concept [19, 38, 49], which provides an explanation for how the central nervous system (CNS) deals with the complexity and high dimensionality of motor control for the musculoskeletal system across multiple degree of freedoms (DoFs) [18]. The concept suggests that the CNS reduces the motor tasks into a lower-dimensional subspace in a modular form. Simply put, the nervous system activates muscles in groups (synergies) for motor control rather than activating each muscle individually. Despite the debate about the neural origin of muscle synergies [6, 33, 48], it has been proved to be useful for many applications such as clinical research [46], prosthesis control [28, 37] and biomechanical studies [35, 36]. In addition, the proposed alternatives to explain the motor control (uncontrolled manifold [40] and an optimal feedback control [43]) have invoked structures that are very similar to muscle synergies [16, 32]. Therefore, the concept of modularity and a combination of shared and task-specific synergies could contribute in motor control as proposed by Bizzi *et al.* [6].

For implementation, two mathematical models have been proposed for the muscle synergy: synchronous model [38, 49] and asynchronous model [19, 20]. The most recent studies relies on the synchronous model since there has been some evidence that muscle synergies are synchronised in time [26, 30]. According to the synchronous model (also known as time-invariant model) the electrical activity for  $j^{\text{th}}$ -muscle or channel  $\mathbf{m}_j(t)$  is a vector that could be expressed as a combination of synchronous synergies  $\mathbf{s}$  scaled by a set of respective weighting functions  $\mathbf{w}_i(t)$  as

$$\mathbf{m}_j(t) = \sum_{i=1}^{i=r} s_{ij} \mathbf{w}_i(t), \quad (1)$$

where  $r$  is the number of synchronous synergies. For a multichannel EMG  $\mathbf{M}$  with  $m$ -channels, equation 1 is expanded into matrix form as

$$\mathbf{M}_{(m \times n)} = \mathbf{S}_{(m \times r)} \times \mathbf{W}_{(r \times n)} \quad (2)$$

with number of synergies  $r$  being restricted to less than number of channels  $m$  ( $r < m$ ) to impose dimension reduction. This is considered as blind source separation problem

where the unknown synergies and their weighting function are estimated from the multichannel EMG signals. In order to estimate the muscle synergies, several matrix factorisation techniques have been explored with NMF [34], PCA [29] and ICA [27] being the most commonly used methods. Among them, NMF is the most prominent and suitable method [22, 47] since the non-negativity constraint makes it more appropriate and easily interpretable because of the additive nature of synergies [8]. However, all these approaches are  $2^{nd}$ -order analysis methods. This may limit them when dealing with situations where repetitive analysis are investigated such as the identification of shared muscle synergies.

The muscle synergies extracted from EMG signals recorded during one motor task can be divided into two groups. The first one is shared, or common, synergies that could be found in another motor tasks sharing some mechanical or physical characteristics with the current one. The other group is task-specific, or behavioural, synergies that are distinctive for that motor task. The existence of these two types of synergies has been observed across species, including frogs [7, 17], cats [44] and humans where different tasks were investigated to identify shared synergies such as walking and cycling [4], postural balance positions [10, 45] and normal walking and slipping [35, 36].

The current approach to estimate the shared and task-specific synergies is applying NMF on the multi-channel EMG signals recorded during the biomechanically-related tasks in question. This is done for several repetitions of each task and usually for a number of different subjects. Then, the synergies are rearranged across tasks, repetitions and subjects (in some cases) in order to maximise the similarity between a set of synergies which is assumed to be shared across tasks and/or subjects. Most of the shared synergies studies rely on correlation coefficients as a similarity metric to identify the shared synergies. Nonetheless, this approach is limited by the fact that the rearrangement of synergies would have a significant effect and impact on this metric [4, 35, 36].

In addition, and as indicated above, the natural structure of data under investigation is not taken advantage of since the procedure involves a repetitive application of analysis steps using  $2^{nd}$ -order model (NMF). Therefore, a higher-order model for muscle synergy would represent the data in a more natural way than the current  $2^{nd}$ -order model. The higher-order model would provide a better alternative to identify shared synergies since it is more natural for the data and will not rely on the similarity via correlation coefficients since the rearrangement process will be skipped. In this case, the data from different repetitions of tasks and subjects would benefit from structuring in an  $3^{th}$ -order tensor form in order to capture the (shared) synergies between tasks. Hence, the second objective of this paper is to utilise the power of tensor decompositions to identify the shared and task-specific synergies between two tasks that forms one degree of freedom (DoF) of wrist movements. A constrained Tucker decomposition method will be developed to identify the shared and task-specific synergies and it will be compared against the current traditional method that uses  $2^{th}$ -order analysis model.

## 2 Materials

In this study, the datasets are selected from the Ninapro first database [2, 3]. The data were collected from 27 healthy subjects. The database includes EMG recordings for 62 wrist, hand and finger movements with 10 repetitions for each movement. The “stimulus” time series in the Ninapro dataset is used to set the segments beginning and end points for each task repetition. Each segment consists of 10-channel signals and rectified by root mean square and sampled at 100Hz.

Biomechanically related tasks/movements were chosen to identify shared and task-specific synergies between them. Related tasks for this study focused specifically

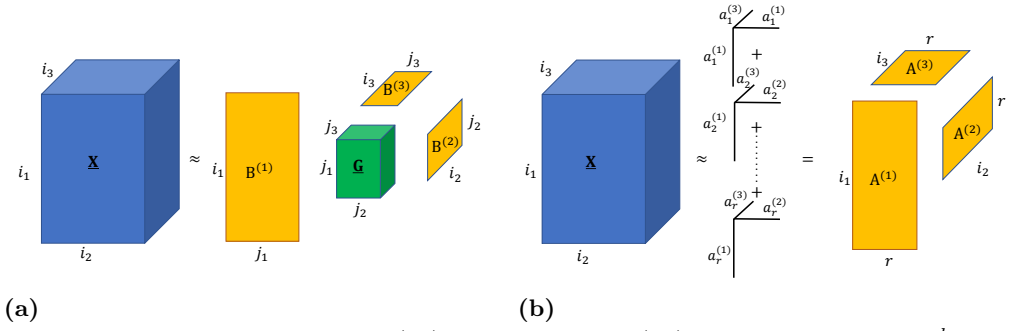


**Figure 1.** Illustration of Tucker (1a) and PARAFAC (1b) decomposition for  $3^{rd}$ -order tensor  $\underline{\mathbf{X}}$ .

on wrist motion and its three Degree of freedoms (DoF). The movements under investigation are: the wrist radial and ulnar deviation that creates the horizontal Degree of freedom (DoF1); wrist extension and flexion movements which form the vertical DoF (DoF2); and finally wrist supination and pronation (DoF3). Each repetition consists of 10-channel recordings of 5s in which the task is executed as illustrated in Figures (2a) and (2b). In order to create a higher order tensor from the data, repetitions from the two biomechanically related tasks are stacked together to form a  $3^{rd}$ -order tensor with modes channels $\times$ time $\times$ repetitions as shown in Figure 2 where a tensor for DoF1 is constructed using repetitions from wrist radial and ulnar deviation multichannel EMG recordings.

### 3 Methods

#### 3.1 Comparison between PARAFAC and Tucker models for muscle activity analysis

##### 3.1.1 Tensor decomposition models

Higher-order tensors can be decomposed into their main components in a similar way to matrix factorisation methods. Several tensor decomposition models have been introduced with Tucker and PARAFAC being the most prominent ones [13]. In Tucker decomposition, the higher-order tensor is decomposed into a smaller core tensor transformed by a matrix across each mode (dimension), where the core tensor determine the interaction between those matrices. On the other hand, PARAFAC could be considered as a special case of Tucker with a supra-diagonal core tensor with 1s across its supra-diagonal and 0s elsewhere which is also known as “identity tensor”. Consequently, the number of components is fixed for all modes for PARAFAC unlike Tucker where the numbers of components in the different modes can differ. Thus, the Tucker model has more flexibility in component number unlike PARAFAC [31]. The differences between both models are represented in Figure 1.

In general, an  $n^{th}$ -order tensor  $\underline{\mathbf{X}} \in \mathbb{R}^{i_1 \times i_2 \times \dots \times i_n}$  can be modelled according to the Tucker model as follows:

$$\underline{\mathbf{X}} \approx \underline{\mathbf{G}} \times_1 \mathbf{B}^{(1)} \times_2 \mathbf{B}^{(2)} \dots \times_n \mathbf{B}^{(n)} \quad (3)$$

where  $\underline{\mathbf{G}} \in \mathbb{R}^{j_1 \times j_2 \times \dots \times j_n}$  is the core tensor and  $\mathbf{B}^{(n)} \in \mathbb{R}^{i_n \times j_n}$  are the components matrices transformed across each mode while “ $\times_n$ ” is multiplication across the  $n^{th}$ -mode [31]. The core tensor  $\underline{\mathbf{G}}$  is flexible to have different dimensions across each mode as long as it is smaller than the tensor being factored,  $\underline{\mathbf{X}}$ , so that  $j_n \leq i_n$ .

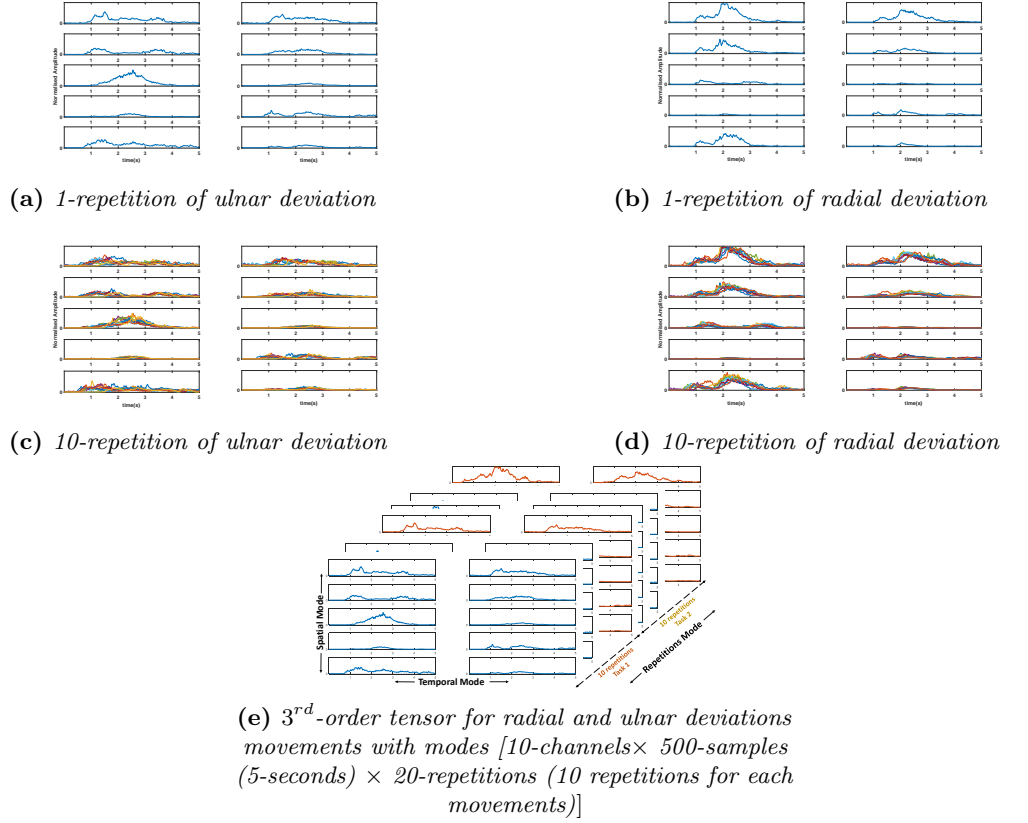


**Figure 2.** An example for data construction and tensor decomposition. Figures 2a and 2b are 10-channel EMG recordings of Ninapro first database (subject 1). The recording is for 1 repetition of ulnar (2a) and radial deviation (2b) movements (DoF1). (Figures 2c and 2d) shows 10 repetitions of each movements, which are stacked together to form  $3^{rd}$ -order tensor as in 2e for DoF1.

On the other hand, PARAFAC approach factorises the  $n^{th}$ -order tensor  $\underline{\mathbf{X}} \in \mathbb{R}^{i_1 \times i_2 \times \dots \times i_n}$  into its component matrices with fixed number of components across each mode as

$$\underline{\mathbf{X}} \approx \underline{\mathbf{A}} \times_1 \mathbf{A}^{(1)} \times_2 \mathbf{A}^{(2)} \dots \times_n \mathbf{A}^{(n)} \quad (4)$$

where  $\underline{\mathbf{A}} \in \mathbb{R}^{r \times r \times \dots \times r_n}$  is a super diagonal tensor that have same dimension across each mode and the vector  $\mathbf{A}$  is across the diagonal of  $\underline{\mathbf{A}}$ . This limits the interactions in-between components unlike Tucker decomposition.

The PARAFAC decomposition is unique under very mild conditions [31]. On the other hand, the Tucker decomposition generally does not provide unique solution [11]. However, the uniqueness can be achieved in practice by imposing additional constraints on the modes [52].

### 3.1.2 Alternating Least Squares algorithm

Both Tucker and PARAFAC can be estimated with the Alternating Least Squares algorithm (ALS), which is used in several matrix factorisation techniques as well. ALS starts initialising the components (and core tensor in the case of Tucker decomposition) to be estimated either randomly or by certain criteria such as singular value decomposition [41]. The next step is to minimise the loss function between the original data and its model by breaking down this complex non-convex problem into a series of

simpler and convex problems tackled in succession [14]. This is done by fixing all the component matrices to be estimated except for those corresponding to one of the modes (dimensions) and alternate iteratively between all the components to solve each convex problem until convergence [12]. Given a  $3^{rd}$ -order Tucker model, equation 3 would be expressed as

$$\underline{\mathbf{X}} \approx \underline{\mathbf{G}} \times_1 \mathbf{B}^{(1)} \times_2 \mathbf{B}^{(2)} \times_3 \mathbf{B}^{(3)} \quad (5)$$

and the least squares loss function for this model would be

$$\underset{\mathbf{B}^{(1)}, \mathbf{B}^{(2)}, \mathbf{B}^{(3)}, \underline{\mathbf{G}}}{\operatorname{argmin}} \|\underline{\mathbf{X}} - \mathbf{B}^{(1)} \underline{\mathbf{G}} (\mathbf{B}^{(3)} \otimes \mathbf{B}^{(2)})^T\|^2 \quad (6)$$

where  $\otimes$  is Khatri-Rao product which is the column-wise Kronecker product. The algorithms in this study are base on an adapted PARAFAC and Tucker functions from the (N-WAY Toolbox) for Matlab [1].

The ALS algorithm has several advantages such as simplicity compared to the simultaneous approaches. However, it is not guaranteed to converge to a stationary point as the problem could have several local minima. Therefore, multiple initialisations and constraints would help to improve the estimation. In tensor factorisation, components could be initialised at random orthogonalised values [25] or by using other methods such as singular value decomposition (SVD) or direct trilinear decomposition (DTD) [39] for a good starting values.

Moreover, constraining the tensor models has several benefits including: improving the uniqueness of the solution, more interpretable results that do not contradict priori knowledge, avoiding degeneracy and numerical problems and speeding up the algorithm. Although constraints could lead to poorer fit for the data compared to the unconstrained model, the advantages outweigh the decrease in the fit for most cases [11]. The decomposition models are constrained through their ALS algorithm in the initialisation and/or updating the components. For example, non-negativity constrained is one of the most commonly used ones due to the illogical meaning for negative components in many cases. The non-negativity constraint is implemented in the updating step by setting the negative values of computed components to zero by the end of each iteration to force the algorithm to converge into a non-negative solution. In the case of muscle synergy extraction, non-negativity would add more information to the decomposition by taking in account the additive nature of muscle synergies.

### 3.1.3 Experimental comparison

To highlight the differences between Tucker and PARAFAC models in muscle activity analysis and synergy extraction, both methods are used to decompose the three  $3^{rd}$ -order tensors of each wrist DoF. A 3-component unconstrained PARAFAC is used for decomposition. The number of components were set to three so that two of them could be dedicated to the two movements forming the DoF and the third would pick up the shared activity between the two tasks. In comparison, a  $[3, 3, 3]$  Tucker decomposition is applied without any constraints on the components or core tensor. The two decomposition methods are applied on each DoF tensor of the three wrist's DoF. The decomposition runs for 10 times on each tensor in order to test if the resulting components can be replicated every run. In other words, to examine the ability of algorithms to converge to the same point and have a unique solution. In addition, the explained variance is recorded to be used as a metric to judge the quality of the decomposition.

## 3.2 Shared synergy identification

The NMF approach to identify the shared synergies from a single task mainly depends on averaging, either by taking the average of all repetitions from a single task and

applying NMF on it or by averaging the synergies extracted from each repetition. The result would be one group of synergies assigned for the task followed by identifying shared synergies by matching the synergies of different tasks according to the correlation coefficient. On the other hand, the tensor approach stacks the repetitions from different tasks together to form a  $3^{rd}$ -order tensor with modes channels $\times$ time $\times$ repetitions as shown in Figure 2. Constrained tensor factorisation is applied on this  $3^{rd}$ -order tensor to extract the shared synergies as well as the task specific ones. This will be discussed in detail in the next sections.

### 3.2.1 Constrained Tucker method

The comparison between Tucker and PARAFAC models encourage us to utilise Tucker decomposition for shared synergy identification since it is better in modelling the DoF tensor (higher explained variance). In addition, Tucker decomposition is preferred for its versatility and flexibility. For instance, by assigning a single component in the temporal mode, information will not be segmented by multiple components as in PARAFAC since we are concerned by the main muscle activity in this case. However, a series of constraints on the decomposition are needed to achieve uniqueness as PARAFAC does. Thus, a  $[1, 3, 3]$  Constrained Tucker decomposition is developed to estimate interpretable components that helps in identifying shared and task-specific synergies.

Constrained Tucker decomposition is utilised to identify shared and task-specific synergies from a  $3^{rd}$ -order tensor with modes (channels  $\times$  time  $\times$  repetitions) where it contains repetitions from two biomechanically related movements (such as ulnar and radial deviation as shown in Figure 2e). There are four main constraints needed to facilitate the shared synergy identification. Two constraints are imposed in the initialisation step on the core tensor and repetitions mode components while the other two are applied during the components update. To link each of the three factors into their respective spatial synergy -either task-specific or shared- the core tensor is initialised and fixed into a value of 1 between each repetition factor and its respective spatial synergy and 0 otherwise. This fixed core set-up and do not update with every iteration. This ensures that every spatial factor is assigned to only one repetition factor and avoid any cross interaction. The values of the core tensor are chosen to be 1 to have all the variability in the components. In addition, Since we know that each repetition belongs to a known movement, the repetitions mode is initialised with three factors (one for each task and the third for the shared synergy). The task-specific factors are designed to have a value of 1 for a repetition of the considered movement and 0 otherwise, while the shared factor is initialised by a value of 0.5 for all repetitions. Unlike the core tensor the update of this mode is not fixed to account for the variability and differences between repetitions of the same movement, alternatively, a controlled averaging constraint is used during the update step.

The other two constraints on updating factors in Tucker’s ALS algorithm are the non-negativity on temporal and spatial modes and the controlled averaging on the initialised repetition mode. The non-negativity constraint are imposed in order to have meaningful factors (synergies) [8, 22] as discussed before. The controlled averaging constraint aims to allow some variability within each repetition factor either it is shared or task specific. This approach will hold the structure of repetition factors that was initialised without fixing it through iterations and take the differences between repetitions into account. This is implemented by modifying the update phase in the ALS algorithm. The estimated factors are averaged after each iteration by a moving average function. This constraint leads to higher explained variance in the Constrained Tucker model compared to fixed factors, thereby improving identification of shared and task-specific synergies.

The constrained Tucker decomposition would result in a shared synergy and 2

task-specific synergies in the spatial mode for  $3^{rd}$ -order tensor with repetitions of 2 tasks (ulnar and radial deviation, for example). As it is common with ALS and tensor decomposition, the algorithm would run for 10 times to ensure that the model is not converged into local minima and the decomposition with the highest explained variance is chosen.

### 3.2.2 NMF as benchmark

NMF [4, 9, 17, 36] is used in this study as a comparative benchmark. NMF processes the multi-channel EMG recording as a matrix  $\mathbf{X}$  with dimensions (channel $\times$ time). NMF decomposes EMG recordings into two smaller matrices (factors). The first factor holds the temporal information (also known as weighting function)  $\mathbf{B}^{(1)}$  while the other is the muscle synergy holding the spatial information  $\mathbf{B}^{(2)}$  as

$$\mathbf{X} \approx \mathbf{B}^{(1)} \times \mathbf{B}^{(2)} \quad (7)$$

where both  $\mathbf{B}^{(1)}$  and  $\mathbf{B}^{(2)}$  are constrained to be non-negative. For details see [21].

Since the dataset had 10 repetitions for each task, NMF was applied on each of them for each task. Number of synergies was chosen by variance accounted for (VAF) as a metric [37]. The first step to identify the shared and task-specific synergies would be finding the reference synergy [4, 36] from the 10 repetitions of that task. This is done by calculating the inter-correlation between the 10 repetitions, and since number of synergies are 2, 200 correlation processes are needed to identify the reference repetition which achieves the highest average correlation coefficient between repetitions. The second step is to use this reference to arrange synergies within each repetition [4]. Finally, the arranged synergies are averaged to compute the first and second mean synergies for the task. Then, to identify the shared synergy of one DoF, the mentioned method is applied on the 2 tasks forming the DoF in question, the correlation coefficients between the resulting 4 mean synergies (2 for each task) are calculated so the highly correlated synergies between the 2 tasks are identified as shared, while the other two are considered as task-specific [9, 36, 45].

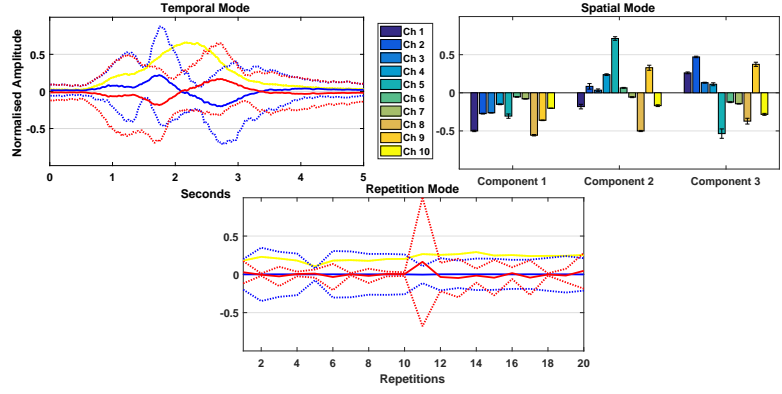
### 3.2.3 Comparison between shared synergies identified by constrained Tucker and NMF

In this study, we compared shared and task-specific synergies identified using the constrained Tucker tensor decomposition method with those identified by using the traditional NMF and correlation method. This comparison is held since there is no ground truth about the shared and task-specific synergies. Therefore, for each wrist's DoF, three synergies are identified by Tucker (2 task-specific and 1 shared synergy) while 4 mean synergies (2 for each task in the DoF) are estimated using NMF. The correlation coefficient between Tucker and NMF synergies are calculated and averaged across all 27 subjects. The comparison is held the main 3 wrist's DoFs: ulnar and radial deviation (DoF1); wrist extension/flexion (DoF2); and wrist supination/pronation (DoF3).

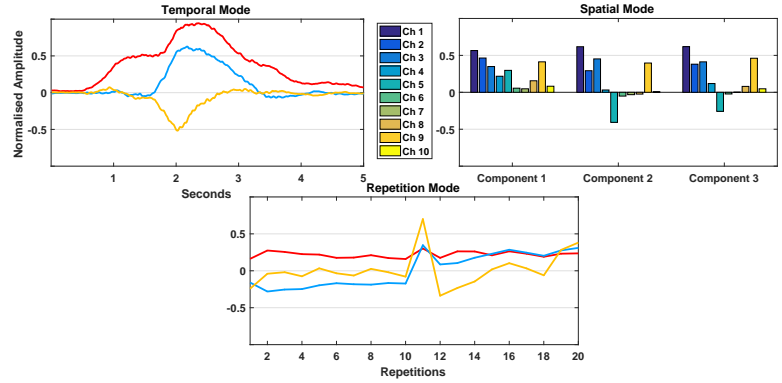
### 3.2.4 Constrained Tucker method validation

In order to provide further validation to the approach of shared synergy identification using constrained Tucker decomposition, the repetition mode in the  $3^{rd}$ -order tensor of each DoF was randomly shuffled to destroy any task-repetition information. The same constrained tucker decomposition algorithm is applied on the tensor to identify shared synergy. The 2 task-specific synergies will be corrupted since information about the tasks are missing. However, this experiment would test the ability of constrained Tucker





(a) The average and standard deviation for 10 runs of unconstrained  $[3, 3, 3]$  Tucker decomposition for DoF1 tensor.



(b) The average and standard deviation for 10 runs of unconstrained 3-components PARAFAC decomposition for DoF1 tensor.

**Figure 3.** The average (solid line) and standard deviations (dotted lines) for 10 runs of unconstrained Tucker (3a) and PARAFAC (3b) applied on the  $3^{rd}$ -order tensor in Fig. 2e. Because of the uniqueness of PARAFAC solution, its standard deviation is zero as shown in Panel 3b. While only one factor (yellow) in Tucker seems to be unique in the temporal and repetition mode as shown in Panel 3a.

method to identify the shared synergies without any data arrangement which cannot be achieved using the traditional NMF and correlation method. The shared synergies identified from the shuffled  $3^{rd}$ -order tensors is compared against the shared synergies estimated from uncorrupted ones by calculating the correlation coefficients between them. The comparison is held using 15 shuffled tensors for each DoF of the main 3 wrist's DoF and the average correlated is computed.

## 4 Results

### 4.1 Comparison between Tucker and PARAFAC tensor decomposition models for muscle activity analysis

An unconstrained 3-component PARAFAC and  $[3, 3, 3]$  Tucker decomposition have been applied on the  $3^{rd}$ -order tensor for DoF1 in (Fig 2e) as well as the other 2 wrist's DoFs tensor for 10 times each. The average explained variance in all Tucker decompositions

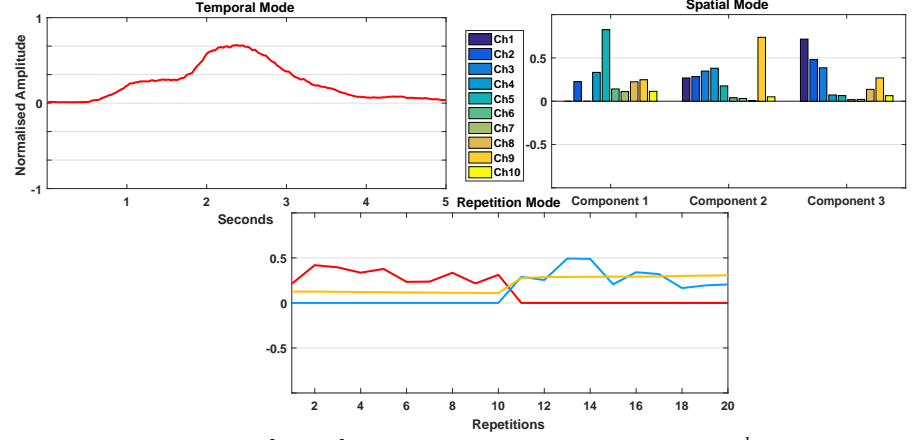


**Figure 4.** Constrained  $[1, 3, 3]$  Tucker decomposition for the  $3^{rd}$ -order tensor in Fig. (2e). The spatial mode had 3 components, the third one represents the shared synergy while other 2 components are task-specific synergies for the ulnar and radial deviation tasks.

was 90.81%. On the other hand, the average explained variance in PARAFAC was lower at 72.63%.

The 10 runs of both decomposition methods for DoF1 tensor of subject “1” (Fig 2) are demonstrated in Figure 3. The mean of the 10 runs is represented by the solid lines while the standard deviations are shown in dotted lines. Since the PARAFAC decomposition usually converges into the same point and its solution is unique, the standard deviation values were nearly zero for 10 runs of the algorithm. On the other hand, despite of the higher explained variance of Tucker, the solution (including the core tensor) was different each run except for one factor (yellow) in the temporal and repetition modes.

## 4.2 Shared synergy identification

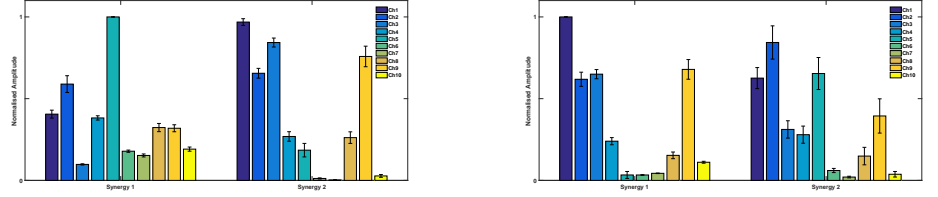
### 4.2.1 Constrained Tucker synergies

The constrained Tucker decomposition was applied on a  $3^{rd}$ -order tensor (Fig 2e) with 10 repetitions from two wrist tasks (1-DoF). The decomposition was constrained to identify the shared synergy between the two tasks and task-specific synergies as well. In Figure 4, a tensor with 20 repetitions of ulnar and radial deviation is decomposed using constrained Tucker. The spatial mode consists of three components the third one is the shared synergy while the first and second components are task-specific synergies for ulnar and radial deviation tasks respectively.

### 4.2.2 NMF synergies

A Number of wrist tasks were selected and 10-channel EMG recording was decomposed using NMF to extract 2 synergies for each task as it was found that 2 synergies would account for over 90% of the variability in data for all repetitions. For each task, NMF was applied on each of the 10 repetitions and the estimated synergies were rearranged using mutual correlation coefficients then averaged across repetitions to result 2 muscle synergies for each movement. An example of the averaged synergies are shown in Figure 5 for the ulnar and radial deviation movements (DoF1) of subject “1”.

Shared synergies are determined through correlation. As shown in Figure 5, the second synergy of ulnar deviation (Fig. 5a) is highly correlated with the first component



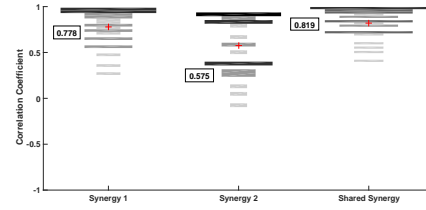
(a)

(b)

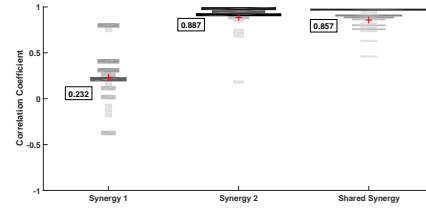
**Figure 5.** 2-component NMF for the ulnar (5a) and radial (5b) deviations movements of subject (1) averaged across 10 repetitions for each task. The second component of ulnar deviation is highly correlated with the first component of radial deviation suggesting that these are the shared synergies between those tasks.

of radial deviation (Fig. 5b) with  $r = 0.91$ . Therefore, according to the standard NMF approach the average of these two synergies is considered as a shared synergy between the ulnar and radial deviation tasks while the remaining synergies are task-specific.

#### 4.2.3 Shared synergies comparison



(a)



(b)

**Figure 6.** Visualisation of the histogram and mean values (red cross) for the correlation coefficients between synergies extracted by constrained Tucker method and NMF averaged synergies for ulnar (Panel 6a) and radial (Panel 6b) deviation (DoF1) for all 27 subjects.

Synergies extracted from constrained Tucker decomposition are compared against NMF synergies to test the ability of this method to identify shared and task-specific synergies. The correlation coefficients between Tucker and NMF synergies is used as a metric. This was done for 3 pairs of tasks (DoFs) for the wrist movements. The average correlations is summarised in table 1. This was done for the 27 subjects in the dataset, where the 3 synergies from Tucker decomposition are compared against each averaged NMF synergies of each task. For example, the correlation coefficients between the estimated tensor synergies and NMF synergies of ulnar and radial deviation for the 27 subjects are represented in Figure 6.

The third (shared) synergy is highly correlated with both tasks as the average correlation coefficients for ulnar and radial deviation are 0.819 and 0.857 respectively.

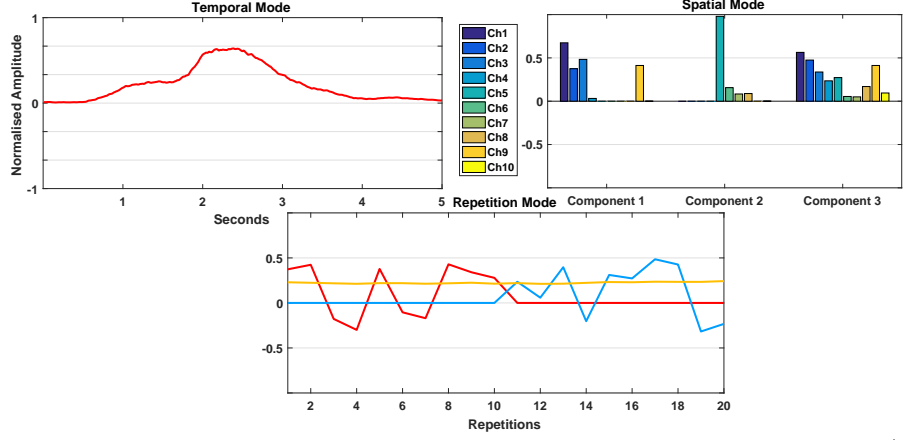


**Figure 7.** Constrained Tucker decomposition for the DoF1 tensor in Figure (2e) but with shuffled repetition mode. The algorithm was able to identify the same shared synergy (third spatial component) as the decomposition of the regular tensor (Fig. 4) even without any task-repetition information.

Each of the other 2 task-specific synergies are correlated with its respective task. For ulnar deviation, the first synergy has correlation coefficient of 0.778 compared to 0.575 for the second synergy, while for the radial deviation the second synergy has an average correlation coefficient of 0.887 compared to 0.232 with the first synergy. Similar results are found with other movements such as wrist extension/flexion and wrist supination/pronation) as shown in Table 1.

#### 4.2.4 Constrained Tucker method validation

In order to validate the approach of shared synergy identification and to show that it is robust to any repetitions disarrangement, the  $3^{rd}$ -order tensor in Figure 2e was randomly shuffled across the repetition mode to destroy the task-repetition information. The constrained Tucker decomposition was applied on the randomly shuffled tensor to identify shared synergy as shown in Figure 7. In comparison with the normal tensor decomposition (Fig. 4), we notice that the task-specific components are different as expected since the information was destroyed. On the other hand, the shared synergy in the spatial mode are very similar. The average correlation coefficients between shared synergies identified from 15 shuffled tensors and from arranged ones are found to be 0.89. This shows the ability of the algorithm to identify the shared synergy despite the corruption in the task-repetition information during the tensor construction unlike NMF method which relies heavily on the data arrangement.

**Table 1.** Average correlation coefficients between Tucker and NMF synergies for the 3 Main DoFs of wrist.

		Synergy 1	Synergy 2	Synergy 3
DOF 1	Ulnar deviation	0.778	0.575	0.819
	Radial deviation	0.232	0.887	0.857
DOF 2	Wrist extension	0.729	0.337	0.868
	Wrist flexion	0.408	0.776	0.880
DOF 3	Wrist supination	0.911	0.481	0.879
	Wrist pronation	0.104	0.920	0.792

---

## 5 Discussion

We proposed and discussed the use of higher-order tensors and their decompositions as a framework to extract muscle synergies from multi-channel EMG signals. This is motivated by the fact that most of EMG datasets are in multi-way form with different repetitions from tasks and/or subjects. However, tensor factorisation has hardly been used in EMG analysis [22]. Our first objective was to demonstrate the use of tensor factorisation in muscle activity analysis by highlighting the differences between PARAFAC and Tucker decomposition models. This was approached by applying both methods without any constraints on  $3^{rd}$ -order tensor consists of 20 multichannel EMG repetitions 2 biomechanically related tasks (10 repetitions each). Our second objective was to develop a constrained Tucker decomposition method to identify task-specific and shared muscle synergies between each pair of tasks that forms a DoF of wrist movements. The resulting synergies were compared against the standard NMF factorisation approach for the 3 wrist's DoFs across 27 subjects.

The comparison between Tucker and PARAFAC decompositions for the estimation of synergies from muscle activity tensors showed the need for additional constraints in order to obtain unique, interpretable and meaningful outputs. For instance, a non-negative constraint is essential because of the additive nature of synergies. The PARAFAC model had a unique solution (even without constraints) and was able to estimate the shared synergy to some extent as shown in Figure 3b where the 1<sup>st</sup> component (red) captured the variability across all 20 repetitions in the repetition mode. Yet, it could not capture the task-specific synergies because it necessarily had to have three components in the temporal mode and this segmented the information of each task's main activity. Even with a non negativity constraint, PARAFAC could not estimate the task-specific synergies. In addition, the percentage variance explained by PARAFAC was about 20% lower than than by Tucker. This percentage dropped further by adding non-negativity constraints. This indicates that the strict PARAFAC model is not suitable to identify both shared and task-specific synergies. On the other hand, unconstrained Tucker decomposition had much higher explained variance (around 90%) but it does not provide a unique solution as shown in Figure 3a. Another problem with unconstrained Tucker in muscle synergy extraction is the core tensor that allows the interactions between all components in each mode. This makes it harder to directly relate synergies (in the spatial mode) to other specific components in temporal and repetition modes. Therefore, Tucker model had to be constrained in order to have a meaningful and unique solution. For instance, In our application to identify shared and task-specific synergies, the  $[1, 3, 3]$  Tucker decomposition algorithm was constrained in the initialisation and iteration stages by imposing constraints on the core tensor and repetition mode in addition to non-negativity. This restricted Tucker decomposition model provided a unique and interpretable solution that identifies shared and task-specific synergies directly despite the fact that additional constraints decreased the average explained variance slightly to 78.2%.

We conclude that constraints play an important role in achieving effective analysis. For instance, the identification of shared and task-specific synergies is not viable by PARAFAC despite having a unique solution. Unconstrained Tucker has higher explained variance but it is not suitable either since its solutions are not unique and hard to interpret. Therefore, a constrained Tucker model is the best model for this application. In this sense, identifying the shared and task-specific synergies across tasks are a good example for utilising the power of tensor decomposition to benefit from the structure of datasets in multi-way form. This is in contrast with the current approaches for shared synergy estimation [4, 9, 10, 35, 36] which apply NMF repetitively on multi-channel EMG recordings of different repetitions and then rely on maximising the correlation coefficients between the estimated synergies with regard to a reference one.

Then, shared and task-specific synergies are identified through the correlation coefficient threshold. In comparison, the constrained Tucker decomposition directly estimate the shared and task-specific synergies in one step. This was illustrated in Figure 4 where component 1 and 2 in the spatial mode are task-specific for the two task forming the tensor while component 3 is the shared synergy between them.

In order to validate the synergies identified via tensor decomposition, we compared them against the synergies extracted using NMF for the 27 subjects. In spite of the potential drawbacks of NMF shared synergies, we used NMF as benchmark since there is no ground truth for shared synergies to compare both methods against. This was done for 3 pairs of tasks (DoFs) for the wrist movements 1. The shared synergies identified by Tucker (third synergy) is highly correlated with both tasks while each of the other two tasks correlates with one task as a task-specific synergy. This highlight the ability of constrained Tucker decomposition to identify task-specific and shared synergies directly from the multi-way datasets. Further validation were held by applying the constrained tucker decomposition on randomly shuffled tensor without any task-repetition information. The algorithm was able to estimate nearly the same shared synergy as the ordered tensor (Figure 7), which indicate robustness of the method. In addition, the standard NMF approaches for shared and task-specific synergies identification are vulnerable to errors and biases since they depend on the particular arrangement of the data, the choice of the reference synergy, and the correlation coefficient threshold. This is not the case for constrained Tucker decomposition approach where it was able to identify the shared synergy even with a shuffled tensor as shown in Fig (7). In addition, it is a more direct and faster alternative since there is no need to apply repetitive NMF and correlation.

Some limitations and future work are worth noting. For instance, further experimenting is needed to include more tasks and datasets especially for the lower limb, since shared synergies are heavily used for the gait and posture analysis [4, 35, 36]. Moreover, extracting muscle synergies using tensor factorisation could be extended to various application by converting the information we have into the right set of constraints. For example, this approach could be extended to estimate the shared synergies across subjects to explore the subject-specific synergies [45] .

## 6 Conclusion

In conclusion, we introduced tensor decompositions (PARAFAC and Tucker) for muscle synergy extraction and described their use in EMG analysis to extract meaningful muscle synergies. A constrained Tucker decomposition method was developed to identify shared and task-specific synergies. The results were validated by comparison against the standard NMF approach using data from the publicly available Ninapro dataset. The constrained Tucker method was more suitable to the multi-way nature of the datasets. Furthermore, it provided more direct and data-driven estimations of the synergies in comparison with NMF-based approaches, making our approach more robust to misarrangements of repetitions and the loss of task-repetition information. Thus, we expect that this study will pave the way for the development of muscle activity processing and analysis methods based on higher-order techniques.

## References

1. C. A. Andersson and R. Bro. The N-way Toolbox for MATLAB. *Chemometrics and Intelligent Laboratory Systems*, 52(1):1–4, Aug. 2000.

2. M. Atzori, A. Gijsberts, C. Castellini, B. Caputo, A.-G. M. Hager, S. Elsig, G. Giatsidis, F. Bassetto, and H. Müller. Electromyography data for non-invasive naturally-controlled robotic hand prostheses. *Scientific data*, 1:140053, Jan. 2014.
3. M. Atzori, A. Gijsberts, I. Kuzborskij, S. Elsig, A. G. Hager, O. Deriaz, C. Castellini, H. Muller, B. Caputo, A.-G. M. Hager, O. Deriaz, C. Castellini, H. Muller, and B. Caputo. Characterization of a benchmark database for myoelectric movement classification. *IEEE Transactions on Neural Systems and Rehabilitation Engineering*, 23(1):73–83, Jan. 2015.
4. F. O. Barroso, D. Torricelli, J. C. Moreno, J. Taylor, J. Gomez-Soriano, E. Bravo-Esteban, S. Piazza, C. Santos, and J. L. Pons. Shared muscle synergies in human walking and cycling. *Journal of Neurophysiology*, 112(8):1984–1998, 2014.
5. H. Becker, L. Albera, P. Comon, M. Haardt, G. Birot, F. Wendling, M. Gavaret, C. G. Bénar, and I. Merlet. EEG extended source localization: Tensor-based vs. conventional methods. *NeuroImage*, 96:143–157, Aug. 2014.
6. E. Bizzi and V. C.-K. K. Cheung. The neural origin of muscle synergies. *Frontiers in computational neuroscience*, 7(April):51, Feb. 2013.
7. V. C.-K. K. Cheung. Central and Sensory Contributions to the Activation and Organization of Muscle Synergies during Natural Motor Behaviors. *Journal of Neuroscience*, 25(27):6419–6434, July 2005.
8. C. Choi and J. Kim. Synergy matrices to estimate fluid wrist movements by surface electromyography. *Medical Engineering and Physics*, 33(8):916–923, Oct. 2011.
9. S. A. Chvatal and L. H. Ting. Common muscle synergies for balance and walking. *Frontiers in computational neuroscience*, 7(May):48, Jan. 2013.
10. S. A. Chvatal, G. Torres-Oviedo, S. A. Safavynia, and L. H. Ting. Common muscle synergies for control of center of mass and force in nonstepping and stepping postural behaviors. *Journal of Neurophysiology*, 106(2):999–1015, Aug. 2011.
11. A. Cichocki, D. Mandic, A. H. Phan, C. Caiafa, G. Zhou, Q. Zhao, and L. De Lathauwer. Tensor Decompositions for Signal Processing Applications From Two-way to Multiway Component Analysis. *IEEE Signal Processing Magazine*, 32(2):1–23, Mar. 2014.
12. A. Cichocki, R. Zdunek, A. H. Phan, and S.-I. Amari. *Nonnegative Matrix and Tensor Factorizations: Applications to Exploratory Multi-Way Data Analysis and Blind Source Separation*, volume 1. John Wiley & Sons, 2009.
13. P. Comon. Tensors : A brief introduction. *IEEE Signal Processing Magazine*, 31(3):44–53, May 2014.
14. P. Comon, X. Luciani, and A. L. de Almeida. Tensor decompositions, alternating least squares and other tales. *Journal of Chemometrics*, 23(7-8):393–405, July 2009.
15. F. Cong, Q.-H. Lin, L.-D. Kuang, X.-F. Gong, P. Astikainen, and T. Ristaniemi. Tensor decomposition of EEG signals: A brief review. *Journal of Neuroscience Methods*, 248:59–69, June 2015.

- 
16. A. Danna-Dos-Santos, E. Y. Shapkova, A. L. Shapkova, A. M. Degani, and M. L. Latash. Postural control during upper body locomotor-like movements: similar synergies based on dissimilar muscle modes. *Experimental brain research*, 193(4):565–79, Mar. 2009.
  17. A. D’Avella and E. Bizzi. Shared and specific muscle synergies in natural motor behaviors. *Proceedings of the National Academy of Sciences of the United States of America*, 102(8):3076–81, Feb. 2005.
  18. A. D’Avella, M. Giese, Y. P. Ivanenko, T. Schack, and T. Flash. Editorial: Modularity in motor control: from muscle synergies to cognitive action representation. *Frontiers in computational neuroscience*, 9:126, Jan. 2015.
  19. A. D’Avella, P. Saltiel, and E. Bizzi. Combinations of muscle synergies in the construction of a natural motor behavior. *Nature neuroscience*, 6(3):300–308, Mar. 2003.
  20. A. D’Avella and M. C. Tresch. Modularity in the motor system: decomposition of muscle patterns as combinations of time-varying synergies. In *Advances in Neural Information Processing Systems 14*, volume 3, pages 141–148. Neural information processing systems foundation, 2002.
  21. K. Devarajan. Nonnegative matrix factorization: an analytical and interpretive tool in computational biology. *PLoS computational biology*, 4(7):e1000029, Jan. 2008.
  22. A. Ebied, L. Spyrou, E. Kinney-Lang, and J. Escudero. On the use of higher-order tensors to model muscle synergies. In *2017 39th Annual International Conference of the IEEE Engineering in Medicine and Biology Society (EMBC)*, pages 1792–1795. IEEE, July 2017.
  23. J. Escudero, E. Acar, A. Fernández, and R. Bro. Multiscale entropy analysis of resting-state magnetoencephalogram with tensor factorisations in Alzheimer’s disease. *Brain Research Bulletin*, 119:136–144, 2015.
  24. R. a. Harshman. Foundations of the PARAFAC procedure: Models and conditions for an “explanatory” multimodal factor analysis. *UCLA Working Papers in Phonetics*, 16(10):1– 84, 1970.
  25. R. A. Harshman and M. E. Lundy. PARAFAC: Parallel factor analysis. *Computational Statistics & Data Analysis*, 18(1):39–72, Aug. 1994.
  26. C. B. Hart and S. F. Giszter. Distinguishing synchronous and time-varying synergies using point process interval statistics: motor primitives in frog and rat. *Frontiers in computational neuroscience*, 7(May):52, Jan. 2013.
  27. A. Hyvärinen and E. Oja. Independent component analysis: algorithms and applications. *Neural Networks*, 13(4-5):411–430, June 2000.
  28. M. Ison and P. Artemiadis. Proportional Myoelectric Control of Robots: Muscle Synergy Development Drives Performance Enhancement, Retainment, and Generalization. *IEEE Transactions on Robotics*, 31(2):259–268, Apr. 2015.
  29. J. E. Jackson. *A User’s Guide to Principal Components*. Wiley Series in Probability and Statistics. John Wiley & Sons, Inc., Hoboken, NJ, USA, Mar. 1991.



30. W. J. Kargo and S. F. Giszter. Individual Premotor Drive Pulses, Not Time-Varying Synergies, Are the Units of Adjustment for Limb Trajectories Constructed in Spinal Cord. *Journal of Neuroscience*, 28(10):2409–2425, Mar. 2008.
31. T. G. Kolda and B. W. Bader. Tensor Decompositions and Applications. *SIAM Review*, 51(3):455–500, Aug. 2008.
32. V. Krishnamoorthy, M. L. Latash, J. P. Scholz, and V. M. Zatsiorsky. Muscle modes during shifts of the center of pressure by standing persons: Effect of instability and additional support. *Experimental Brain Research*, 157(1):18–31, Oct. 2004.
33. J. J. Kutch and F. J. Valero-Cuevas. Challenges and new approaches to proving the existence of muscle synergies of neural origin. *PLoS computational biology*, 8(5):e1002434, Jan. 2012.
34. D. D. Lee and H. S. Seung. Learning the parts of objects by non-negative matrix factorization. *Nature*, 401(6755):788–91, Oct. 1999.
35. G. Martino, Y. P. Ivanenko, A. D’Avella, M. Serrao, A. Ranavolo, F. Draicchio, G. Cappellini, C. Casali, and F. Lacquaniti. Neuromuscular adjustments of gait associated with unstable conditions. *Journal of Neurophysiology*, 114(2011):jn.00029.2015, Sept. 2015.
36. M. M. Nazifi, H. U. Yoon, K. Beschorner, and P. Hur. Shared and Task-Specific Muscle Synergies during Normal Walking and Slipping. *Frontiers in Human Neuroscience*, 11(February):1–14, Feb. 2017.
37. G. Rasool, K. Iqbal, N. Bouaynaya, and G. White. Real-Time Task Discrimination for Myoelectric Control Employing Task-Specific Muscle Synergies. *IEEE transactions on neural systems and rehabilitation engineering*, 24(1):98–108, Jan. 2016.
38. P. Saltiel, K. Wyler-Duda, A. D’Avella, M. C. Tresch, and E. Bizzi. Muscle synergies encoded within the spinal cord: evidence from focal intraspinal NMDA iontophoresis in the frog. *Journal of neurophysiology*, 85(2):605–619, Feb. 2001.
39. R. Sands and F. W. Young. Component models for three-way data: An alternating least squares algorithm with optimal scaling features. *Psychometrika*, 45(1):39–67, Mar. 1980.
40. J. P. Scholz and G. Schöner. The uncontrolled manifold concept: Identifying control variables for a functional task. *Experimental Brain Research*, 126(3):289–306, May 1999.
41. A. Smilde, R. Bro, and P. Geladi. *Multi-Way Analysis with Applications in the Chemical Sciences*. John Wiley & Sons, Ltd, Chichester, UK, Aug. 2004.
42. L. Spyrou, S. Kouchaki, and S. Sanei. Multiview Classification and Dimensionality Reduction of Scalp and Intracranial EEG Data through Tensor Factorisation, Aug. 2016.
43. E. Todorov and M. I. Jordan. Optimal feedback control as a theory of motor coordination. *Nature neuroscience*, 5(11):1226–1235, Nov. 2002.

- 
44. G. Torres-Oviedo, J. M. Macpherson, and L. H. Ting. Muscle synergy organization is robust across a variety of postural perturbations. *Journal of neurophysiology*, 96(3):1530–1546, Jan. 2006.
  45. G. Torres-Oviedo and L. H. Ting. Subject-Specific Muscle Synergies in Human Balance Control Are Consistent Across Different Biomechanical Contexts. *Journal of Neurophysiology*, 103(6):3084–3098, June 2010.
  46. D. Torricelli, F. Barroso, M. Coscia, C. Alessandro, F. Lunardini, E. Bravo Esteban, and A. D’Avella. Muscle Synergies in Clinical Practice: Theoretical and Practical Implications. In J. L. Pons, R. Raya, and J. González, editors, *Emerging Therapies in Neurorehabilitation II*, volume 10 of *Biosystems & Biorobotics*, pages 251–272. Springer International Publishing, Cham, 2016.
  47. M. C. Tresch, V. C.-K. K. Cheung, and A. D’Avella. Matrix factorization algorithms for the identification of muscle synergies: evaluation on simulated and experimental data sets. *Journal of neurophysiology*, 95(4):2199–2212, Apr. 2006.
  48. M. C. Tresch and A. Jarc. The case for and against muscle synergies. *Current Opinion in Neurobiology*, 19(6):601–607, Dec. 2009.
  49. M. C. Tresch, P. Saltiel, and E. Bizzi. The construction of movement by the spinal cord. *Nature neuroscience*, 2(2):162–7, Feb. 1999.
  50. L. R. Tucker. Some mathematical notes on three-mode factor analysis. *Psychometrika*, 31(3):279–311, Sept. 1966.
  51. P. Xie and Y. Song. Multi-domain feature extraction from surface EMG signals using nonnegative tensor factorization. In *2013 IEEE International Conference on Bioinformatics and Biomedicine*, pages 322–325. IEEE, Dec. 2013.
  52. G. Zhou and A. Cichocki. Fast and unique Tucker decompositions via multiway blind source separation. *Bulletin of the Polish Academy of Sciences: Technical Sciences*, 60(3):389–405, Jan. 2012.